PROFILE DESIGN AND CFD EVALUATION OF VARIOUS SUPERSONIC NOZZLE CONFIGURATIONS

L. DAI[1]*, N. BORDJIBA[2], A. HADDAD[3]

In the field of aerodynamics, supersonic flows play a significant role due to their unique properties and innovative applications. This work focuses on the design and analysis of de-Laval type supersonic nozzles using the Method of Characteristics (MoC) and Computational Fluid Dynamics simulation with ANSYS-Fluent. Three types of profiles are designed and simulated: the classic conical contour, the more advanced contour known as the bell-shaped profile, and finally a more daring contour generally referred to as an open nozzle. The profiles of the different divergent sections are simulated by a straight line, a second-degree polynomial, and an exponential function respectively. The convergent section is the same for all profiles as it serves solely to expand the flow to reach subsonic speeds at the throat, and is profile is designed through the application of Rao method. The obtained results, based on pressure and Mach contours as well as performance characteristics, demonstrate the superiority of the bell-shaped profile compared to the other two nozzle designs.

Keywords: Supersonic propulsion nozzles, Method of characteristics, Supersonic design, Subsonic design, CFD, Ansys-Fluent.

1. Introduction

Nozzles are devices that transform thermal energy into kinetic energy without any moving parts. The profile of supersonic nozzles significantly impact several key performance parameters [1]. Their contour development has been a progressive evolution driven by advancements in aerodynamics, propulsion systems, and aerospace engineering. Integrating a combustion chamber within a C-D nozzle leads to achieving very high speeds that may reach Mach 7 [2].

The development of C-D nozzles of conical shape has been pivotal in the advancement of supersonic propulsion technology. They are characterized by their simple and straightforward conical shape. However, they tend to be longer than other designs, leading to increased weight and hence performance loss at low altitude. Supersonic conical nozzles have been the subject of numerous studies based on their design and optimization, considering both their geometry and suitability for integration into rockets designed for high-altitude flights [3-4].

[1] *PhD student, LMANM, FST, 8 May univ., Algeria, e-mail: lyliadai66@gmail.com (corresponding author)
[2] MSc student, Dept of Mech Eng., 8 May univ., Algeria, e-mail: bourdjiba395@gmail.com
[3] Prof., LMANM, FST, 8 May univ., Algeria, e-mail: haddad.abdelkrim@univ-guelma.dz

Besides the aforementioned conical nozzle, which typically features a straight-walled design with a 15° angle of divergence, the method of characteristics (MoC) was predominantly used in the design of other configurations. Among them, the contoured nozzle that features a bell-shaped or flared design that gradually widens from the throat to the exit. In contrast to the conical nozzle, which maintains a constant divergent angle, the bell-shaped nozzle features a varying expansion angle that starts between 20° and 50° immediately downward of the throat. This is accompanied by a progressive contour adjustment, reducing the gradient to reach an approximate half-angle of 5°-10° at the ejection edge. Contoured nozzles have been found to be around 20% shorter in length and consequently lighter [5]. In terms of shortcomings, the design and manufacturing of such configurations are more complex compared to conical nozzles. Their precise contour requires advanced engineering and manufacturing techniques, which can be more costly and time-consuming. [6]

Introducing an arc-based contour design, Alili et al. [7] compared it to a conventional conical nozzle. The contoured configurations, designed using the MoC, demonstrated superior performance with increases of up to 11% in thrust.

Various nozzle configurations, such as expansion-deflection (E-D), dual bell, and plug profiles have been proposed with the primary goal of maximizing thrust while minimizing overall length [8]. Among them, the so-called open nozzle has been chosen to be investigated. Seldom encountered in the specialized bibliography, such configurations are designed to allow fluids to exit freely without the formation of shock waves typically associated with C-D nozzles. Silva and Brójo [9] presented a noteworthy review of diverse nozzle configurations highlighting advancements in rocket propulsion efficiency. Their study employs both the MoC and CFD simulations to analyze conical, bell, aerospike, and E-D configurations.

Nowadays, modern computer platforms integrate the MoC as one of numerical tools to solve differential equations. Its contemporary significance in supersonic and hypersonic nozzle design has been demonstrated [10]. Direct methods of optimization emerged, such as the one using 2^{nd}-order polynomial contours that could achieve comparable maximum thrust nozzle profiles [11].

The present research investigates the extension of simulating supersonic nozzle contours using profile relationships. The nozzle contour is mathematically represented by a straight line for conical nozzles, a 2^{nd}-degree polynomial for bell-shaped nozzles, and a mathematical exponential function to describe open nozzles. The subsonic section, shared by all three configurations, is designed using the experimental approach introduced by Rao [12]. The transonic flow-field is analyzed using perturbation and series expansion theories [13], while the supersonic flow is computed using the MoC. The flow-fields within the three nozzle configurations obtained are subsequently simulated using Ansys-Fluent

software [14], and the results obtained are compared. Contoured nozzles are found to exhibit superior performance than to conical and open configurations.

2. Design and simulation

2.1 Supersonic section design: the characteristics approach

The mathematical representation of a 2-D, steady, isentropic, and irrotational flow is governed by nonlinear differential equations of the potential of velocity, as expressed in equations (1) to (3) [6].

$$\left(u^2-a^2\right)\frac{\partial u}{\partial x}+\left(v^2-a^2\right)\frac{\partial v}{\partial y}+2uv\frac{\partial u}{\partial y}-\delta\frac{a^2 v}{y}=0 \tag{1}$$

$$\frac{\partial u}{\partial y}-\frac{\partial v}{\partial x}=0 \tag{2}$$

$$a=a\ (u,v) \tag{3}$$

The MoC, implemented within a custom-developed program[15], was used to design the supersonic section to meet the specified geometric and thermodynamic requirements listed in Table 1.

Table 1

Thermodynamic and geometrical inputs

Ambient pressure, P_a	1.013×10^5 Pa	Throat radius		0.088 m
Total pressure, P_t	54×10^5 Pa	Upstream radius of curvature		0.176 m
Total temperature, T_t	2500 K	Downstream radius of curvature		0.044m
Specific gas constant, R_G	280 J/kg.K	Attachment and Exit angles	Conical	$\theta_A=\theta_E=10°$
			Contoured	$\theta_A=20°$; $\theta_E=5°$
			Open	$\theta_A=15°$
Specific heat capacity ratio, γ	1.2	Exit cross-section radius, y_E		0.197m

In the present investigation, the divergent sections are modeled using three distinct profiles, each defined by its respective mathematical relationship. A program using the Fortran language and incorporating the MoC procedure, has been developed and utilized for this purpose. The conical, contoured and open nozzle profiles are approximated by a straight-line, a 2nd-degree polynomial, and by an exponential (Equations 4, 5 and 6 respectively). In addition to the relationships describing the three profiles, the equations present the parameters that define these correlations.

$$y=A_w+B_w x\ ;\ A_w=y_A-x_A\cdot tg\left(\theta_A\right)\ \text{and}\ B_w=tg\left(\theta_A\right) \tag{4}$$

$$y = A_w + B_w x + C_w x^2 \; ; \begin{cases} A_w = y_A - \dfrac{x_A^2 \cdot tg(\theta_E) - 2x_A x_E \cdot tg(\theta_A)}{2(x_A - x_E)} \\ B_w = \dfrac{x_A \cdot tg(\theta_E) - x_E \cdot tg(\theta_A)}{(x_A - x_E)} ; C_w = \dfrac{tg(\theta_A) - tg(\theta_E)}{2(x_A - x_E)} \end{cases} \quad (5)$$

$$y = A_w e^{B_w \cdot x} \; ; A_w = \exp\left[Ln(y_A) - \frac{x_A \cdot tg(\theta_A)}{y_A} \right] \text{ and } B_w = \frac{tg(\theta_A)}{y_A} \quad (6)$$

Finally, the divergent sections of the three nozzle configurations may be drawn. They are constituted of two arcs of circle, the one downstream of the throat being linked to either a straight line, a 2nd-order polynomial or an exponential contour.

The convergent section is designed to accelerate the flow to transonic velocities at the throat allowing for a supersonic expansion afterwards and is common to all three profiles. The Rao method [12] is applied to outline this section profile whose axial (x) and radial (y) coordinates are expressed by Equations (7) and (8), and whose contour is depicted in Figure 1.

$$x = 1.5\, y_t \cos(\theta) \; ; \quad (7)$$

$$y = 1.5 y_t \sin(\theta) + 2.5 y_t \quad (8)$$

with: $\theta \leq -90°$ and $\theta \geq -130°$

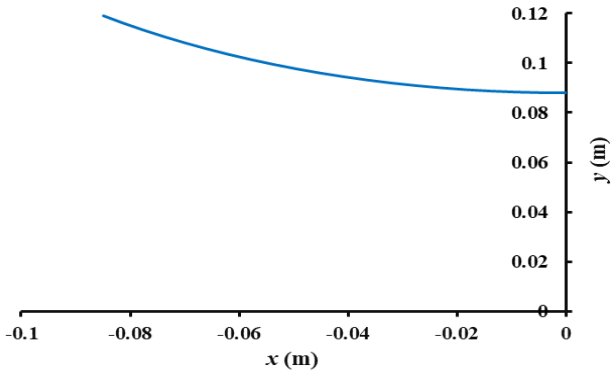

Fig. 1. Divergent section profiles applicable to all three profiles

Finally, the full profiles of the three nozzle configurations are developed. They are illustrated in Figure 2. These profiles will be incorporated into the Fluent

software to simulate the flow fields occurring within the convergent, throat, and divergent sections.

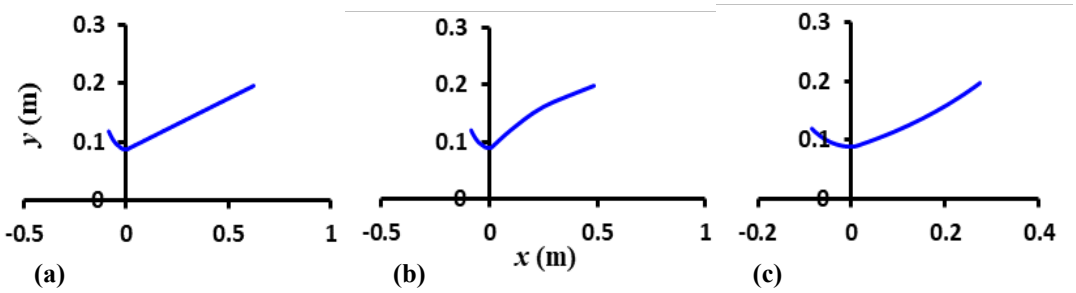

Fig. 2. Divergent section profiles (a) conical, (b) contour, (c) open

3. CFD computations

3.1 Domain discretization and mesh independence

The choice of a computational domain spatial grid resolution greatly influences the final solution. While a finer grid results in only minor variations in the fundamental flow structure, it significantly raises computational expenses. Therefore, an optimal grid should strike a balance between precision and computational efficiency. A grid independence study was therefore conducted on the contoured nozzle, which represents the most geometrically complex configuration among the three studied designs. Three different mesh densities were tested: a coarse grid (100×30), a medium grid (200×60), and a fine grid (300×90), corresponding to total cell counts of 3,000, 12,000, and 27,000 within the nozzle, respectively. The obtained results, in terms of mass flow rate and developed thrust, are summarized in Table 2.

Table 2

Comparison of coarse, medium, and fine meshes

Mesh Size	Mass flow rate (kg/s)	Thrust (N)
100×30	102.85	186,742.89
200×60	104.23	190,183.25
300×90	104.43	190,881.62

In terms of developed thrust, the comparison reveals a notable increase in thrust between the coarse and medium mesh (approximately 1.8%), while it equals 0.37% when medium and fine grids are compared. In terms of mass flow rate, the same trend may be noticed.

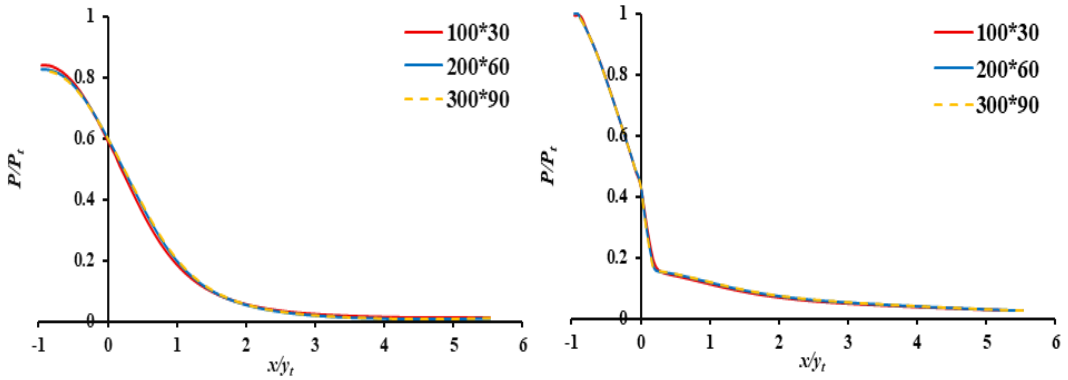

Fig. 3. Dimensionless pressure distributions along (a) the centerline and (b) the wall, using three levels of grid resolution

The results reveal that the medium and fine grids produce identical pressure distributions, whether along the centerline or wall along the supersonic section (Figure 3). However, the coarse mesh shows differences at the beginning of the expansion process. Given the close agreement between the medium and fine grids, the former grid (i.e. 200x60) was selected for subsequent simulations to optimize computational resources. In this setup, the mesh was refined near the nozzle walls, ensuring a dimensionless wall distance (Y^+) of unity.

3.2 Grid topology

In order to maintain consistency and ensure comparable resolution near critical regions, the validated mesh parameters were adapted to the other two configurations, ensuring that the flow results can be fairly compared between the different geometries, while keeping the numerical results reliable. Figure 4 illustrates the grid topology employed for the three configurations.

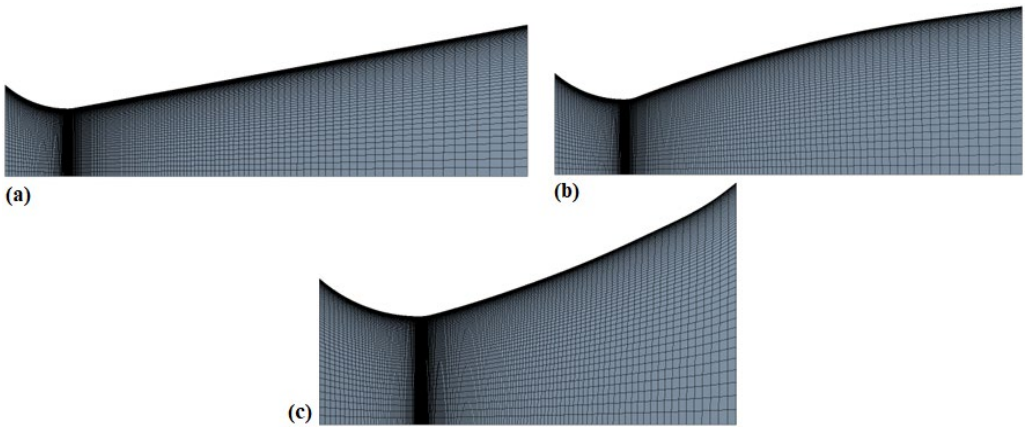

Fig. 4. Grid topology of nozzles (a) conical, (b) contour, (c) open

the Reynolds-Averaged Navier–Stokes (RANS) equations for turbulent flow were solved in order to investigate the compressible flow within the three nozzle configurations [16]. To achieve system closure, the turbulence effects were accounted for using the *k-ω* sst two-equation turbulence model. This model, known for its robustness in capturing near-wall flow features is particularly suited for the transonic and supersonic regimes involved in nozzle internal flow [17]. The combination of RANS equations with the *k-ω* sst model ensured a balanced trade-off between computational efficiency and predictive accuracy, thereby providing reliable estimates of flow characteristics such as pressure fields, and thrust performance across the studied geometries. The specific computational factors utilized for computer modeling are presented in Table 3.

Table 3

Configuration parameters for nozzle modeling

	Implemented characteristics
Framework	2D, steady-state, Compressible viscous medium
Algorithm	Density-driven
Eddy viscosity closure	*k*-omega sst
Medium	Perfect gas (air)
Input parameters	54.10^5 Pa / 2500 K
Output parameters	$1.013.10^5$ Pa
Residual	10^{-5}

As indicated in Table 3, the residual was set to 10^{-5}. The computational steps number needed to achieve the desired solution was found equal to 2114 for the conical case. For the contoured and open configurations case, the convergence was reached for 2076 and 2139 iterations respectively.

4. Results and discussion

The simulations were conducted in 2-D, with a focus on the wall and centerline distributions of pressure aimed at the three configurations. Primary performance parameters considered include thrust (T), thrust coefficient (C_T), mass flow rate ($\dot{m}$), specific impulse (I_S), effective velocity (V_{eff}), and exit Mach number (M_e).

4.1 Pressure profiles

Figure 5 illustrates the centerline and wall distributions of pressure for the three configurations investigated. It shows a rapid decrease in pressure along the axis and the wall, with both profiles converging at the exit. In the case of the conical geometry (Figure 5-a), the pressure along the wall is found to be slightly higher. The open nozzle indicates a rapid decrease in pressure (Figure 5-c), more

pronounced than in the conical and contour configurations represented in Figure 5-a and Figure 5-b. This setup seems to facilitate faster and less controlled gas expansion, especially near the walls.

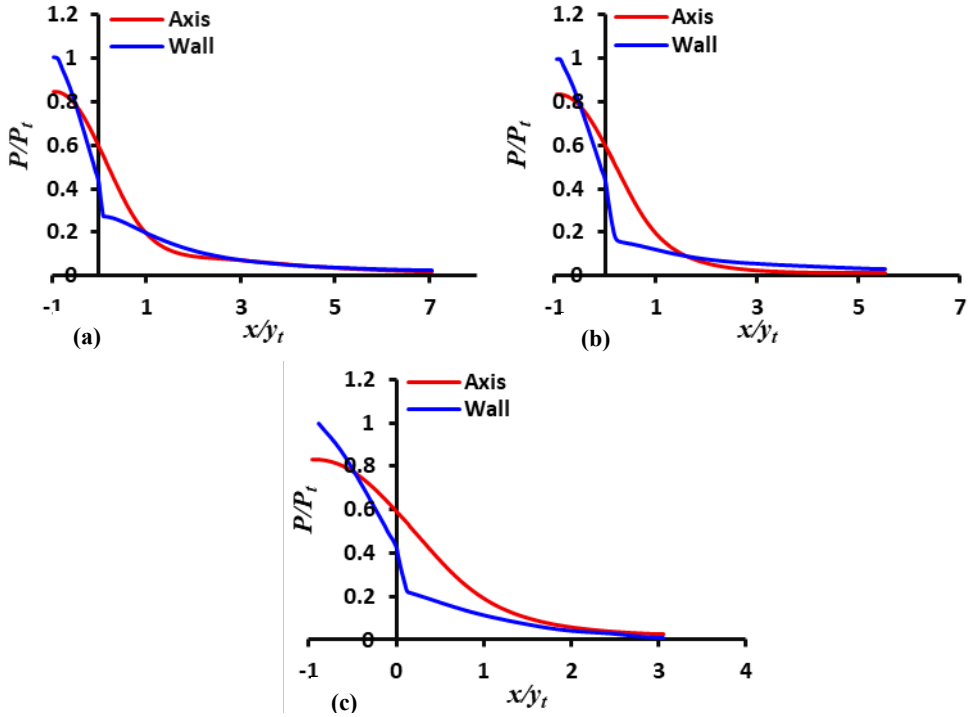

Fig. 5. Wall and centerline distributions of pressure for (a) conical, (b) contour, (c) open

4.2 Pressure and Mach contour distributions

The same trend observed in the pressure distribution (Figures 5) is reflected in the contours. The expansion starts straight from the entrance and is initiated at the subsonic section. It continues until the nozzle exit. (Figure 6). In the case of the conical configurations with its 10° divergence angle, the pressure transition is relatively smooth and linear (Figure 6-a). However, and regarding the contour nozzle, the 20° attachment angle induces a relatively rapid initial expansion which is later followed by a smoother one due to the 5° exit angle (Figure 6-b). The curvature and angles result in greater pressure variations compared to the conical configuration. In the open configuration represented in Figure 6-c, the pressure drops rapidly, accompanied by an abrupt transition. The 15° attachment angle and the exponential profile allow for a swift gas expansion, leading to a quick pressure decrease. The short length of the nozzle promotes rapid diffusion but can result in efficiency loss. There is a fast transition from subsonic to supersonic speeds.

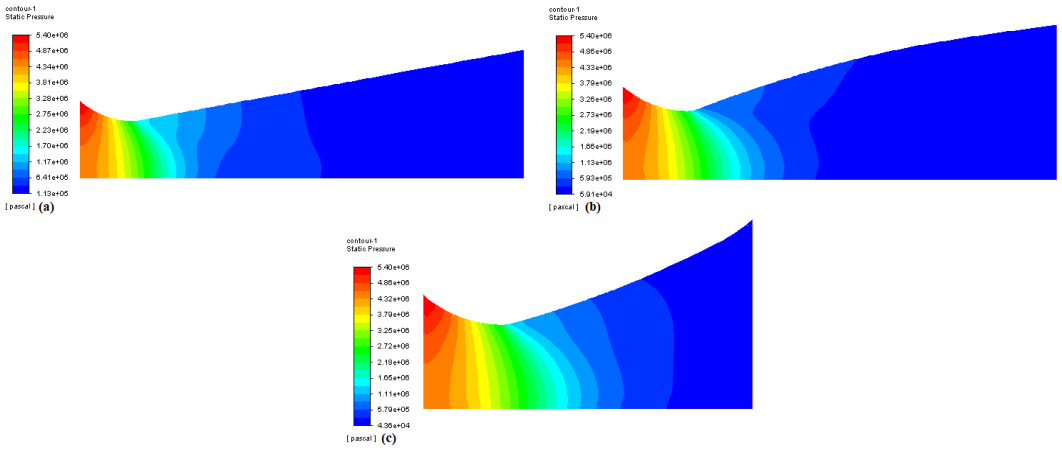

Fig. 6. Pressure contours along nozzles (a) conical, (b) contour, (c) open

In terms of Mach number, the relatively long length of the conical configuration (Figure 7-a) seems to facilitate a smooth increase in Mach. This design is well-suited for applications that require stable flow and a gradual reduction in pressure. When it comes to the contour profile (Figure 7-b), the Mach number increases more significantly due to both its curvature and larger attachment angle (20°). The color transitions in the contour configuration indicate a rapid acceleration downstream of the throat followed by a gradual stabilization toward the outlet. The contoured nozzle, with its attachment angle and (5°) exit angle, effectively achieves supersonic speeds quickly while controlling the velocity distribution to minimize losses. Being the shortest between the three configurations, the open nozzle achieves a rapid acceleration (Figure 7-c) leading it to be suitable for applications requiring rapid expansion. It needs adjustments to minimize thrust loss due to divergence at the exit.

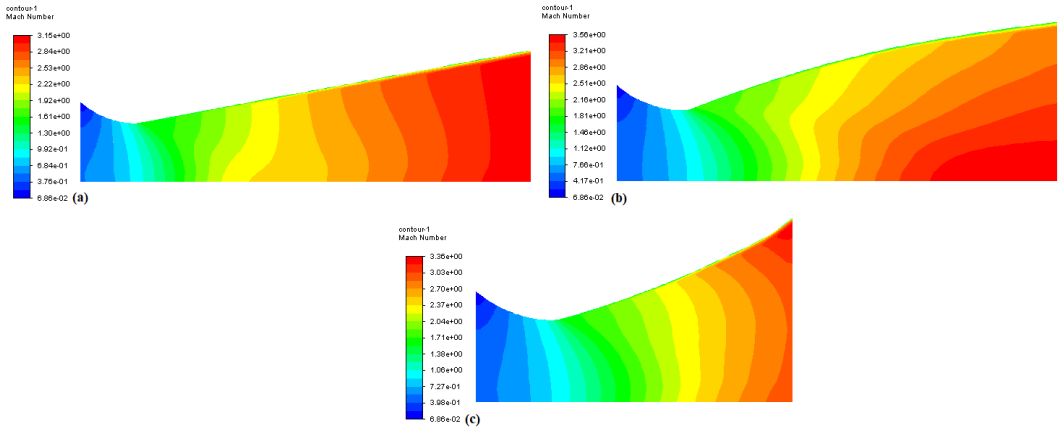

Fig. 7. Mach contours along nozzles (a) conical, (b) contour, (c) open

4.3 Performance

The performance parameters of the different configurations are represented in Table 4. The contoured nozzle is found to develop the highest thrust, mainly because of its directing of the exiting flow. It is followed by the conical nozzle, and far behind the open configuration.

Table 4

Nozzle performance parameters

Performance parameters	Conical nozzle	Contoured nozzle	Open nozzle
Thrust, T (N)	189,583.45	190,183.25	181,677.86
Mass flow rate, $\dot{m}$ (kg/s)	104.23	104.23	104.23
Thrust coefficient, C_T (-)	1.44	1.45	1.38
Specific impulse, I_s (s)	185.41	186.09	177.68
Effective velocity, V_{eff} (m/s)	1818.9	1824.6	1743.05
M_{exit} (-)	3.08	3.06	2.99

Concerning the coefficient of thrust that indicates the effectiveness of supersonic expansion control, the open nozzle underperforms while the contoured nozzle exhibits the best control with $C_T = 1.45$. Although the open nozzle achieves the highest effective velocity, this advantage is offset by significant flow exit divergence that affects the thrust in the axial direction.

In terms of Mach, both the conical and contoured nozzles exhibit nearly identical exit Mach values. However, the contoured nozzle attains this value (M_{exit}=3.06) in a more compact design, resulting in a lighter device. The open nozzle, on the other hand, lags significantly behind in performance.

4. Conclusions

Recent advancements in propulsion technology are closely linked to significant progress in both nozzle contour design and aero-thermodynamic analysis phenomena within propulsion nozzles, particularly within their supersonic sections. Achieving higher exit Mach numbers and significant thrust in the most compact and lightweight configurations depends on optimizing the performance of all engine components, with the nozzle playing a crucial role in generating propulsion thrust. The present research aims to further the understanding of simulating supersonic nozzle contours using standard equations to define their profiles. Specifically, the nozzle contours have been modeled as a straight line, a 2nd-degree polynomial and an exponential function for conical, contoured and open configurations respectively. Subsonic and transonic profiles are determined using methods based on Rao's experimental and perturbation-series theories, respectively, while the supersonic section is developed using the

method of characteristics. Furthermore, CFD simulations have been conducted using the Ansys-Fluent platform in order to analyze the flow within all the three configurations. The RANS relationships have been employed, complemented by the sst k-ω model of turbulence to achieve closure.

The conical configuration is found to offer stability and a gradual expansion, making it an optimal choice for missions requiring a smooth transition. Its length enables consistent pressure management, reducing friction and gas deflection effects. In contrast, the contoured nozzle, with its complex profile and specific attachment and exit angles, facilitates faster acceleration immediately downstream of the throat and allows for controlled gas expansion. This minimizes losses, particularly those due to divergence, making it ideal for applications needing high thrust. The open nozzle, being the shortest of the three, promotes rapid acceleration, reflected by a quick increase in Mach number and a corresponding rapid drop in pressure. However, this leads to a less controlled transition. While it provides rapid acceleration, it may suffer from efficiency losses, making it suitable for missions requiring quick adjustments and short maneuvers.

The comparative analysis concludes that the contoured configuration emerges as the best option. Its relatively short length and therefore a favorable weight, combined with high thrust effectively maximizes the performance of propulsion nozzles, providing an optimal balance between rapid acceleration, controlled gas expansion, and minimized thrust losses due to divergence. Moreover, it offers a balanced compromise between the other two profiles, enabling rapid acceleration and controlled gas expansion, while also delivering the highest thrust. This combination of performances makes it the most suitable profile for rocket engines and space vehicles, maximizing efficiency and overall performance.

Acknowledgement

The present research has been undertaken at the 8th May 1945 Univ of Guelma, Algeria, as part of the PRFU project of research A11N01UN240120210001. The authors extend their sincere appreciation to the DGRSDT for their valuable support.

REFERENCES

[1] *J. L. Turner*, Rocket and spacecraft propulsion: principles, practice and new developments, Springer Science & Business Media, 2008.
[2] *P. Jayaprakash, D. Dhinarakaran, and D. Das*, Design and analysis of a rocket C-D nozzle, International Journal of Health Sciences, **6(S5)**, 3545–3559, 2022.
[3] *M. R. Haque, W. Asrar, and S. Gupta*, A review of conical supersonic nozzle design and optimization, Aerospace Science and Technology, **115**, 106267, 2021.

[4] *R. Nalim, G. S. Samuelsen*, Conical nozzle design for high-altitude rocket flights, Aerospace Science and Technology, **80**, 253-260, 2018.
[5] *T. Elnady, W. Shyy*, Recent advances in contoured supersonic nozzle design and optimization. Progress in Aerospace Sciences, **119**, 100668, 2021.
[6] *B. Kumar, M. Shoaib, G. Ramanan, and P. Rahakrishnan*, Design and Computational Flow Analysis of Different Rocket Nozzle Profile, ACS Journal for Science and Engineering, **2.2**, 49-60, 2022.
[7] *N. Alili, A. Benouar, M. A. Djeffal, K. Kaddouri, K., & M. Salem*, Novel Circular Arc Contour Design for Optimizing Rocket Nozzle Efficiency. Journal of Aeronautics, Astronautics and Aviation, **56(4)**, 801-809, 2024.
[8] *S. Khare, U. K. Saha*, Rocket nozzles: 75 years of research and development, Sådhanå, **46(76)**, 2021.
[9] *J. C Silva, F. Brójo*, A Review on Supersonic Nozzle Design and Analysis with Traditional Methods, Preprints.org, 2025.
[10] *J. C Silva, F. Brójo*, Contemporary importance of the method of characteristics for supersonic nozzle design, Evolutions Mech. Eng., **5(4)**, 2024.
[11] *J. G. Allman, J. D. Hoffman*, Design of maximum thrust nozzle contours by direct optimization methods, AIAA journal, **19(6)**, 750-751, 1981. Published Online: 17 May 2012.
[12] *D. Y. K. Uyeki*, A design method for a supersonic axisymmetric nozzle for use in wind tunnel facilities, MSc in Aerospace Eng, Dept of Aerospace Eng, Dan José University, **201**, 2018.
[13] *J. R. Kliegel, J. N. Levine*, Transonic flow in small throat radius of curvature nozzles, AIAA Journal, **7(7)**, 1375-1378, 1969. Pub. online: 17 May 2012.
[14] *ANSYS, Inc*., Fluent, Release 21.2, ANSYS, Inc., 2022.
[15] *M. K. Elshebani, E. I. Dekam*, A MOC-Based Software; Design and Evaluation of Converging Diverging Nozzles, Journal of Engineering Research, 21-44, 2020.
[16] *G. Scarlatella, J. Sieder-Katzmann, M. Propst, T. Heutling, J. Petersen, F. Weber, ..., C. Bach*, RANS Simulations of Advanced Nozzle Performance and Retro-Flow Interactions for Vertical Landing of Reusable Launch Vehicles, Aerospace (MDPI Publishing), **12(2)**, 2025.
[17] *R. S. Raman, S. V. Kumar, U. Reddy, A. Dodke, A. Kumar, S. Jayronia, M. M. Adnan*, Design and CFD Simulation of Supersonic Nozzle by Komega turbulence model for Supersonic Wind Tunnel. In E3S Web of Conferences, **507**, EDP Sciences, 2024.